HYDROLOGY OF FRITCHIE MARSH, COASTAL LOUISIANA

By Eve L. Kuniansky

U.S. GEOLOGICAL SURVEY

Water-Resources Investigations Report 84-4324

Prepared in cooperation with

LOUISIANA DEPARTMENT OF ENVIRONMENTAL QUALITY
OFFICE OF WATER RESOURCES

Baton Rouge, Louisiana

1985

UNITED STATES DEPARTMENT OF THE INTERIOR

DONALD PAUL HODEL, Secretary

GEOLOGICAL SURVEY

DALLAS L. PECK, Director

For additional information
write to:

District Chief
U.S. Geological Survey
P.O. Box 66492
Baton Rouge, LA 70896
(Telephone: (504) 389-0281)

Copies of this report can be
purchased from:

Open-File Services Section
Western Distribution Branch
U.S. Geological Survey
Box 25425, Federal Center
Denver, CO 80225
(Telephone: (303) 236-7476)

CONTENTS

ILLUSTRATIONS

[Plates are at back]

TABLES

FACTORS FOR CONVERTING INCH-POUND UNITS TO INTERNATIONAL SYSTEM (SI) OF METRIC UNITS

Multiply	By	To obtain
cubic foot per second (ft^3/s)	0.02832	cubic meter per second (m^3/s)
foot (ft)	0.3048	meter (m)
foot per second (ft/s)	0.3048	meter per second (m/s)
mile (mi)	1.609	kilometer (km)
mile per hour (mi/h)	1.609	kilometer per hour (km/h)
million gallons per day (Mgal/d)	0.04381	cubic meter per second (m^3/s)

National Geodetic Vertical Datum of 1929 (NGVD of 1929): A geodetic datum derived from a general adjustment of the first-order level nets of both the United States and Canada, formerly called mean sea level. NGVD of 1929 is referred to as sea level in this report.

HYDROLOGY OF FRITCHIE MARSH, COASTAL LOUISIANA

By Eve L. Kuniansky

ABSTRACT

A preliminary study of Fritchie Marsh near Slidell, Louisiana, was conducted to determine its general hydrology. The marsh is being considered as a disposal site for sewage effluent from the city of Slidell. Knowledge of the effects of specific locations of the sewage outfall to provide maximum mixing and detention time in the marsh is needed. Mixing and detention capabilities of the marsh are dependent upon the flow characteristics for various hydrologic conditions. Model results and field data indicate that, during neap tide with little or no rain, large parts of the marsh are stagnant; and sewage effluent, at existing and projected flows, has minimal effect on marsh flows. During a high tide with a 0.5-foot tide differential across the marsh, steady-state simulations indicate very low velocities with less stagnant water in the marsh.

INTRODUCTION

Fritchie Marsh, 6 mi southeast of Slidell, in southeastern Louisiana, is being considered as an alternative disposal site for treated domestic sewage. Knowledge of the effects of specific locations of the sewage outfall to provide maximum mixing and detention time in the marsh is needed. Mixing and detention capabilities of the marsh are dependent upon the flow characteristics for various hydrologic conditions.

The U.S. Geological Survey, in cooperation with the Louisiana Department of Environmental Quality, Office of Water Resources,[1] has performed a preliminary study for determining general hydraulic characteristics of the marsh system that are significant in selecting locations for effluent discharge and transport in the marsh. A mathematical model was developed along with data-collection procedures for future model calibration and postconstruction monitoring. The two-dimensional FESWMS program (finite-element surface-water modeling system) was used for modeling the marsh. This report presents the first application of the FESWMS program to a marsh system and illustrates the usefulness of the two-dimensional program for studying the marsh.

---

[1] Formerly the Department of Natural Resources, Water Pollution Control Division.

The study area is bounded by U.S. Highway 190 on the north and east, U.S. Highway 90 on the south and east, and Louisiana Highway 433 on the west and south (fig. 1). The two major channels in the marsh are drainage canal W-14 and Salt Bayou. Drainage canal W-14 is the principal storm-runoff drain for Slidell and also carries treated domestic sewage from the Slidell area into Salt Bayou through Little Lagoon, near the bridge opening at Louisiana Highway 433 (fig. 2). The west end of Salt Bayou connects to Lake Pontchartrain and the east end connects to the lower Pearl River basin. Inflows and outflows to the marsh at both ends of Salt Bayou are tidally controlled, and the water is normally brackish.

A coarse finite-element network was developed for modeling Fritchie Marsh; the grid was detailed in the vicinity of canal W-14 and Salt Bayou. Limited field data were collected for developing the model and understanding the hydrology of the marsh, but the data were not adequate for rigorous model calibration. Four hypothetical simulations were made using the following boundary conditions:

1. Sustained neap (low) tide and no wind with minimum effluent in canal W-14.
2. Sustained neap tide and no wind with maximum effluent in canal W-14.
3. Sustained high tide and stage differential with minimum effluent in canal W-14.
4. Sustained high tide with stage differential with maximum effluent in canal W-14.

All simulations were considered as steady-state events. Tidal stage and inflow could be transient between simulations but not during simulations. Steady-state simulations demonstrate possible flow distributions created by prolonged high or low tides but are not adequate to determine the assimilation capability of the marsh. This initial modeling effort was designed to provide insight in the planning of future hydrodynamic simulations of the marsh system.

The assistance of Charles Palmisano, St. Tammany Parish Mosquito Abatement District 2, in providing access to the marsh for data collection, is gratefully acknowledged.

DESCRIPTION OF THE FRITCHIE MARSH FLOW SYSTEM

The Fritchie Marsh flow system is a hydraulically complex system. The variables affecting flows into and out of the marsh are rainfall, runoff, sewage effluent, gravity tides, and wind-driven currents. This part of the report has been divided into two sections. The first section describes the significant physical features of the marsh that affect flow. The second section describes the hydrology of the marsh as determined from the field data collected and from other studies of the surrounding area (Cardwell and others, 1967; Lee and others, 1983).

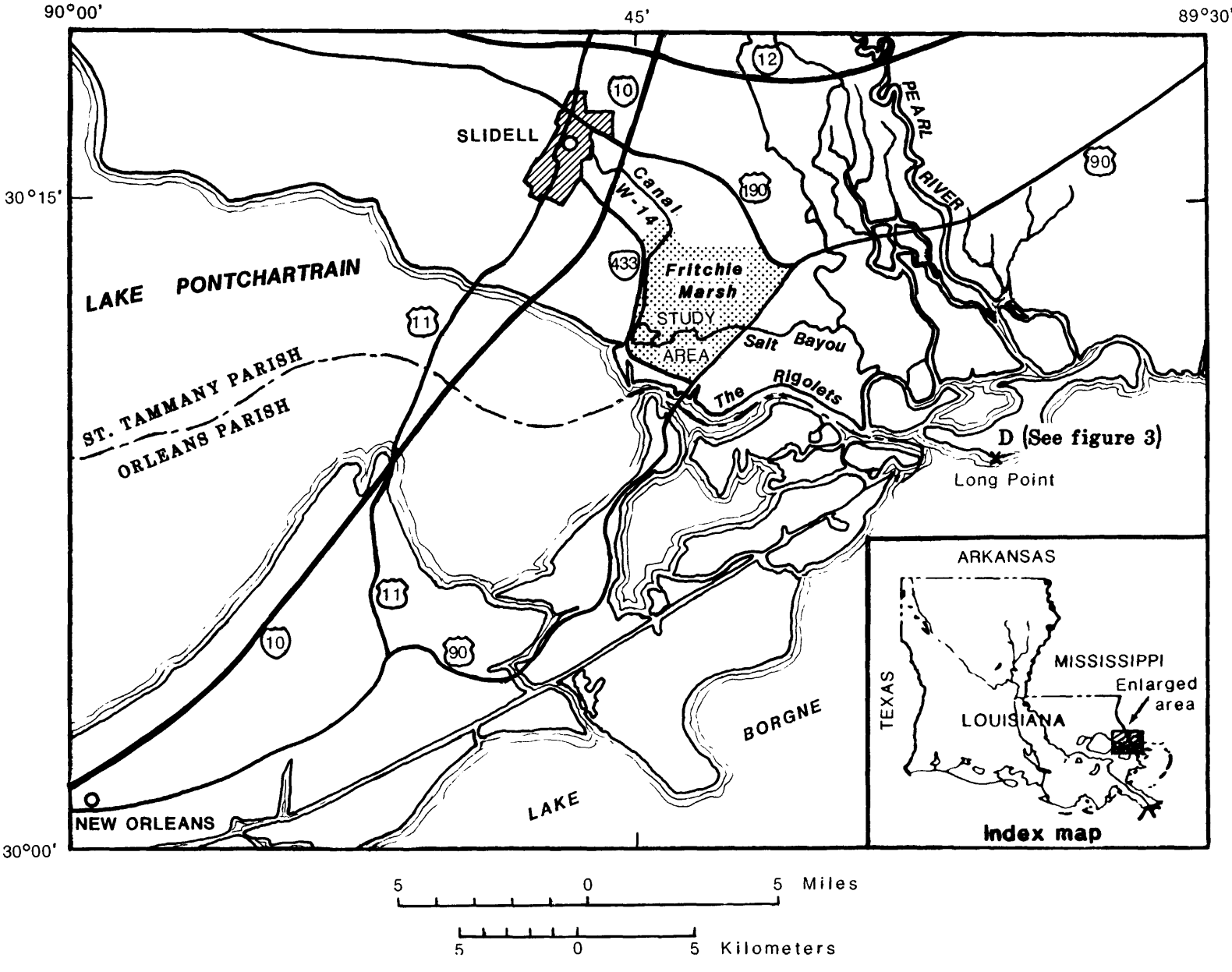

Figure 1.--Location of the Fritchie Marsh and surrounding area.

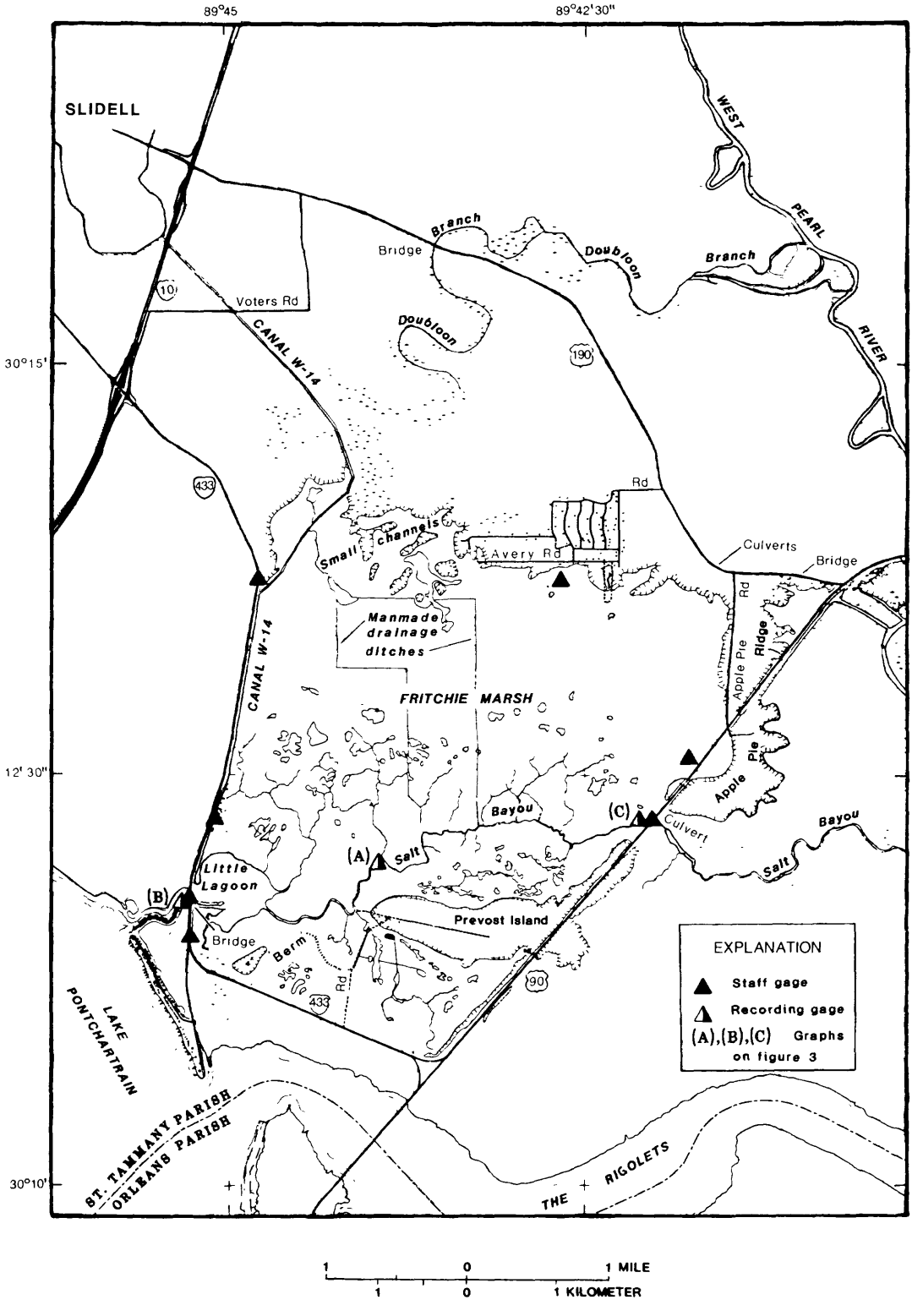

Figure 2.--Significant features of Fritchie Marsh.

Significant Features

The physical features that affect flow are inlets and outlets, channel locations, geometry of the marsh, island locations, and vegetation. The marsh has three major inlets and outlets and several minor ones. The two major channels are Salt Bayou and canal W-14. The geometry of the channels and marsh was determined by field measurements made during the week of August 22-26, 1983. The marsh contains several islands and a small lagoon. Vegetation is varied in the different areas of the marsh. The significant features are discussed in some detail, following, and are shown in figure 2.

The three major points of inflow and outflow for the marsh are canal W-14, at the northwest side of the marsh; the east end of Salt Bayou, which connects to the West Pearl River through a 6-foot concrete box culvert at U.S. Highway 90; and the west end of Salt Bayou, which connects to Lake Pontchartrain through a 170-foot bridge opening in Louisiana Highway 433 at Little Lagoon. Freshwater from storm runoff, base flow, and treated domestic sewage from Slidell enter the marsh through canal W-14, which is always a source of inflow. The two ends of Salt Bayou are tidally affected and flows have been observed both into and out of the marsh at these two locations. The salinity of the water entering the marsh at either end of Salt Bayou varies but is normally brackish.

Minor points of inflow into the marsh are culverts and bridges in the U.S. Highway 190 embankment. Doubloon Branch, predominantly a cypress swamp located east of canal W-14, is a minor inlet to the marsh. Doubloon Branch carries water into the marsh from the West Pearl River during high stages. The water enters the marsh through a 60-foot bridge opening in the U.S. Highway 190 embankment (fig. 2). The elevation of the bed of Doubloon Branch is about 0.5 ft above sea level; the width varies from about 500 to 1,500 ft. There are four culverts at the bend in the highway between Avery Road and the intersection of U.S. Highways 190 and 90. These culverts allow flow to enter the marsh during heavy rainfall and high stages on the lower Pearl River. All four culverts are 60 ft in length, three are oval metal culverts 3 ft in height and 4.5 ft in width, and one is a rectangular concrete culvert 2 ft high and 4 ft wide. Another 60-foot bridge opening on U.S. Highway 190 is located 1,500 ft west of the intersection of U.S. Highways 190 and 90. This bridge spans a small unnamed slough which is ponded except during high stages of the West Pearl River.

The marsh contains two major channels and many minor channels. The major channels are canal W-14, which runs from the north along the west side of the marsh to Little Lagoon, and Salt Bayou, which runs east to west across the southern part of the marsh. Canal W-14 is fairly uniform in geometry, the width varies from 60 to 100 ft and the channel-bed elevations vary (in mid-channel elevation) from 3.5 to 7 ft below sea level. There is a flow restriction in canal W-14, 0.5 mi northeast of where the canal parallels Louisiana Highway 433 and southwest of the two small channels that leave canal W-14 (fig. 2). The canal width narrows to 70 ft at this location and has a bed elevation of 3.5 ft below sea level. Salt Bayou is

120 ft wide at the east side of Little Lagoon and narrows to 30 ft near the east side of the marsh at the culvert. The bed elevation of Salt Bayou varies from 4.3 to 7.4 ft below sea level. Two small, man-made drainage canals in the marsh are 5 ft wide and have a bed elevation of 1 ft below sea level. Many smaller natural channels in the marsh connect to Salt Bayou and canal W-14 (fig. 2).

The vegetation along the border of the southern parts of the marsh is predominantly saltmarsh grass. Freshwater vegetation predominates at the northwest corner of the marsh. The north-central part of the marsh has a bed elevation of approximately 0.5 ft below sea level and is either open water or covered by lilies. The smaller channels connect this central pond-like region with Salt Bayou.

Two large islands in the southern part of the marsh are tree covered and are connected by a berm. A road from Louisiana Highway 433 to Prevost Island, the larger island, separates a corner of the marsh from the main part of the marsh (fig. 2).

Little Lagoon, on the west end of Salt Bayou near the bridge opening on Louisiana Highway 433, varies in bottom elevation from 2 to 8 ft below sea level. The outfall of canal W-14 is at the northwest side of Little Lagoon, north of the bridge opening in Louisiana Highway 433 (fig. 2).

Hydrology of Fritchie Marsh

The movement of water in Fritchie Marsh is complicated by the number of meteorological variables controlling flows. The most significant variables affecting flows in the marsh are rainfall, runoff, winds, gravity tides, stage of the West Pearl River, floods in the lower Pearl River basin, and sewage effluent.

During the April 1983 flooding of the lower Pearl River basin, two measurements of flows into Fritchie Marsh were taken along U.S. Highway 190 (table 1). At Doubloon Branch, 2,530 ft^3/s was measured flowing into the marsh through the bridge opening in U.S. Highway 190. At the bend in U.S. Highway 190, where the four culverts are located, 8,447 ft^3/s was measured flowing over the road. The April 1983 flood is the largest flood of record on the lower Pearl River. According to residents along Avery Road, which borders the northeastern side of the marsh, water flowed overland across Avery Road and Apple Pie Road (fig. 2) into the marsh during this flood.

During the week of August 22-26, 1983, when field data were collected, there was very little wind and no rain. Velocities were too slow in canal W-14 and at the bridge at Louisiana Highway 433 on Salt Bayou to make discharge measurements on August 26, 1983. Discharge into the marsh at the 6-foot box concrete culvert at the intersection of Salt Bayou and U.S. Highway 90 was measured at 3.8 ft^3/s on August 26, 1983 (table 1). No water from Doubloon Branch flowed into the marsh. Like Doubloon Branch, none of the culvert openings in the U.S. Highway 190 embankment had water flowing into Fritchie Marsh during this week. Water-surface elevations in the marsh were observed at 1.0 ± 0.3 ft above sea level during this week.

Table 1.--Stage and discharge measurements around Fritchie Marsh

Location	Conditions	Date (1983)	Stage above sea level (feet)	Direction of flow	Discharge (cubic foot per second)
Doubloon Branch and U.S. Highway 190.	Pearl River flood.	Apr. 6	----	South	2,530
Bend in U.S. Highway 190 where four culverts are located.	Pearl River flood, measurement of flow over U.S. Highway 190.	Apr. 6	----	South	8,447
Salt Bayou and box culvert at U.S. Highway 90.	Neap tide, no wind.	Aug. 26	----	West	3.8
Salt Bayou and bridge at Louisiana Highway 433.	No rain, neap tide, no wind.	Aug. 26	----	-----	(a)
Canal W-14 and Voters Road.	--do----	Aug. 26	----	-----	(a)
Salt Bayou and box culvert at U.S. Highway 90.	No rain, some wind.	Oct. 25	0.80	East	12
Salt Bayou and bridge at Louisiana Highway 433.	--do----	Oct. 25	1.90	West	531
Canal W-14 and Voters Road.	--do----	Oct. 25	----	South	23

[a] Not measured; observed as too small to measure.

On October 25, 1983, stage and discharge measurements were made at both ends of Salt Bayou (table 1) and at canal W-14 at Voters Road. No significant rainfall occurred in the Slidell area during the 2 weeks prior to these measurements. A flow of 23 ft^3/s was measured entering the marsh through canal W-14 at Voters Road; 12 ft^3/s was flowing out of the marsh through the culvert in Salt Bayou at U.S. Highway 90; and 531 ft^3/s was flowing out of the marsh through the bridge opening at

Salt Bayou and Louisiana Highway 433 (table 1). The measurements on canal W-14 at Voters Road and on Salt Bayou at Louisiana Highway 433 were rated as poor measurements due to the slow velocities and the length of time of the measurements. Sewage effluent was discharged upstream of Voters Road into canal W-14 after the beginning of the measurement and the tide was rising at Louisiana Highway 433. The discharge measured at Salt Bayou at U.S. Highway 90 was rated as a good measurement. It also should be noted that high and low tides did not occur according to tidetable predictions on either October 24 or 25, 1983.

Treated domestic sewage entered the marsh through canal W-14 at an average rate of 5.7 Mgal/d (8.8 ft^3/s of discharge) in 1983, which has a minimal impact on flow velocities in the marsh.

During the week of December 13-20, 1983, three continuous-recording stage gages were placed along Salt Bayou (fig. 2), at the east and west ends of Salt Bayou and midway in the marsh. Water-surface elevations plotted at 2-hour intervals for the week of December 13-20, 1983, are shown in figure 3. The curve shown in figure 3d is the predicted gravity-tidal fluctuations for Long Point on Lake Borgne for the same period.

The marsh is in a microtidal zone where gravity-tidal fluctuations are less than 2 ft. Figure 4 shows the gravity tides adjusted to Long Point on Lake Borgne near Fritchie Marsh for the month of August 1983. The gravity tides are diurnal and neap tides occur every 14 days. Neap tides last 3 to 4 days during which there is little gravity-tidal fluctuation. Neap tides occurred August 26-29. Little or no breeze was observed at the marsh on August 26; therefore, there was no wind-induced flow or stage fluctuation at the marsh. By comparing the graphs in figure 3, it can be seen that the eastern end of Salt Bayou (fig. 3c), which is connected to the West Pearl River, has more distinct gravity-tidal fluctuations than the western end of Salt Bayou (fig. 3b), which is connected to Lake Pontchartrain. The water-surface fluctuations midway in the marsh along Salt Bayou (fig. 3a) have a response more similar in shape to the fluctuations for the west end of Salt Bayou (fig. 3b). The diurnal gravity tides are not as apparent in figures 3a and 3b as in figures 3c and 3d. There is a time lag in water-surface fluctuations at the three points in the marsh. The graph in figure 3a shows fluctuations occurring approximately 2 hours after similar fluctuations shown in figure 3b for the west end of Salt Bayou and the amplitude of the fluctuations are not as large at the mid-marsh site. Fluctuations at the mid-marsh site (fig. 3a) appear to lag about 4 hours behind the water-surface fluctuations shown in figure 3c for the east end of Salt Bayou.

The actual water-surface elevations at Fritchie Marsh (fig. 3) are not very similar to the elevations of the gravity tides of the area shown in figures 3d and 4. Other forces in addition to gravity, such as wind, must be affecting the tides. Winds blowing in one direction over a large body of water will cause the water surface to slope upward in the direction the wind is moving. This sloping water surface can be significant due to the large reach of the body of water. The east end of Salt Bayou

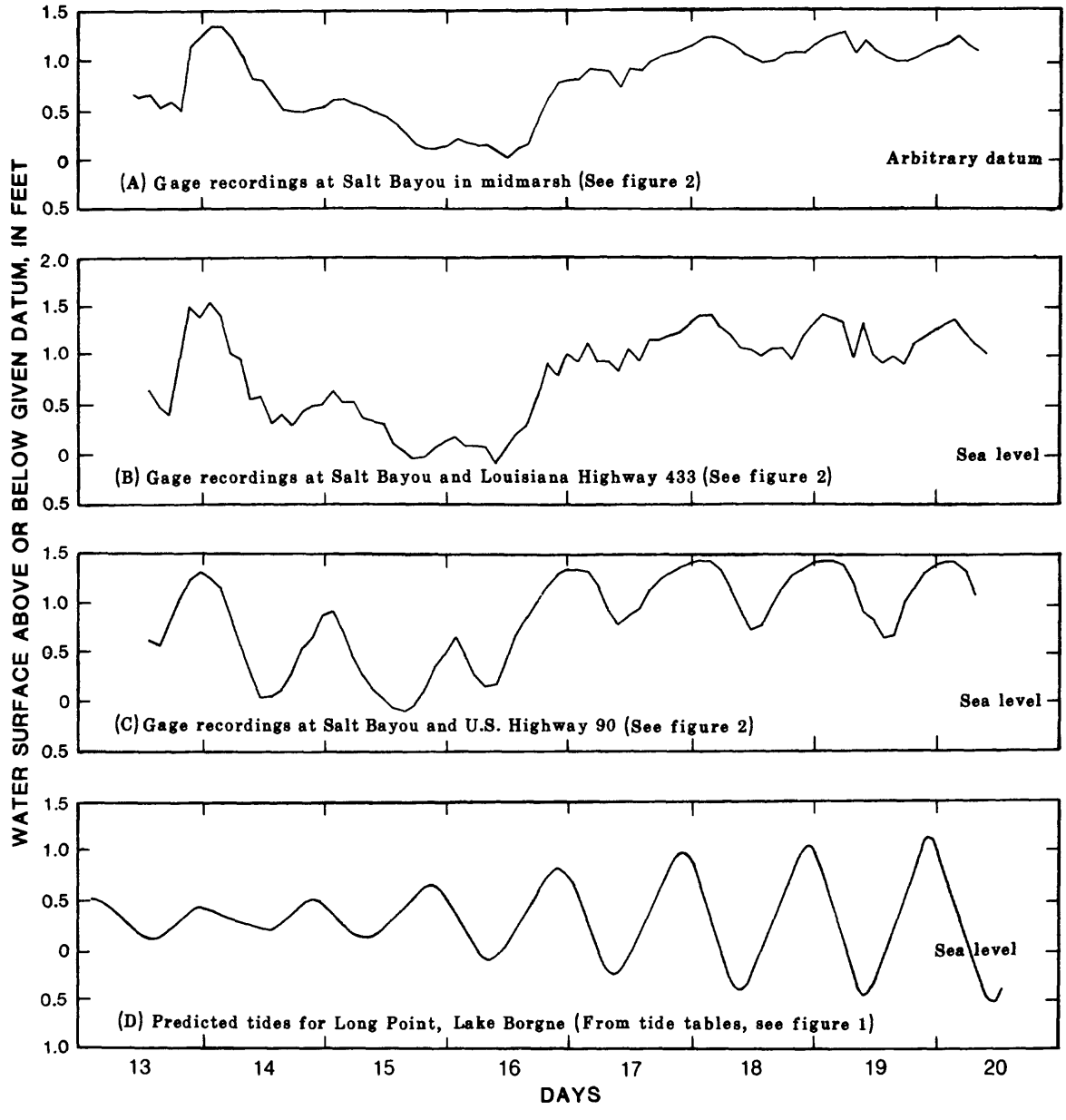

Figure 3.--Water-surface elevations at four locations, December 13-20, 1983.

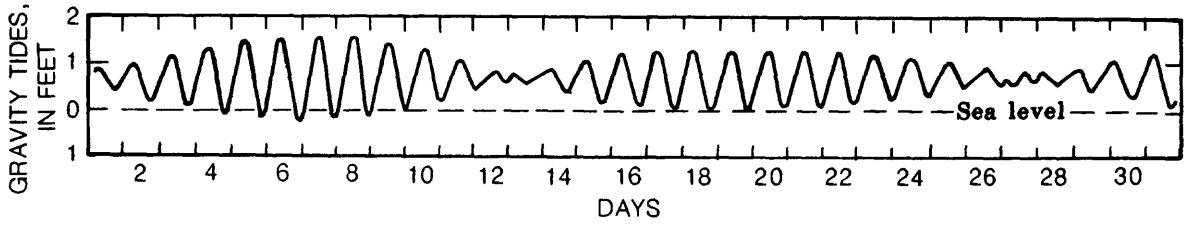

Figure 4.--Predicted gravity tides at Long Point on Lake Borgne near Fritchie Marsh, August 1983.

is connected to the Gulf of Mexico through the West Pearl River, Lake Borgne, and the Mississippi Sound. The marsh is also connected to Lake Pontchartrain and Lake Borgne through The Rigolets. Lake Pontchartrain is approximately 41 mi long from east to west and 25 mi wide from north to south. The Rigolets channel is approximately 0.5 mi wide at each end and is aligned in an east-west direction. Lake Borgne is 26 mi long, 11 mi wide, and is oriented southwest-northeast. The Mississippi Sound is oriented east-west (out of map area). All of these bodies of water are large enough for wind-shear forces to create significant changes in water surface. In this microtidal region, a strong wind of long duration could create more water-surface fluctuation than the gravity tide, depending on the direction of the wind.

Table 2 shows hourly wind data recorded December 13-20, 1983, at the New Orleans International Airport, approximately 35 mi southwest of Fritchie Marsh. The hourly wind record for December 13 shows that some fairly strong winds were blowing from the southeast. The winds shifted direction and blew from the west and northwest from the evening of December 13 through December 14. Winds from the southeast would cause a build-up of water on the northwest side of the Mississippi Sound near the mouth of the Pearl River and in Lake Pontchartrain, raising water levels in the marsh; whereas, winds from the west should lower the water surface at the mouth of the Pearl River and Lake Pontchartrain.

December 13-15 was a neap-tide period, but the water surface in the marsh rose when the wind was from the southeast and declined when the wind was from the west (figs. 3a and 3b). Wind velocities were sporadic December 15, but continued to blow from the west or southwest. Water levels in the marsh continued to decline.

The wind shifted direction blowing from the east and northeast from December 16-20, 1983. A corresponding (figs. 3a and 3b) rise in water surface at the marsh occurred over that period of time. From comparison of the wind data with the stage data in figure 3, it can be concluded that strong winds from the east tend to cause a rise in water surface, and winds blowing from the west tend to lower the water surface at Fritchie Marsh.

Inflows and outflows for the marsh are tidally controlled at the east and west ends of Salt Bayou. Water-surface elevations, however, are more dominated by wind forces than gravitational forces. During heavy rains and floods in the lower Pearl River basin, large amounts of freshwater may enter the marsh from both rain and runoff. During neap-tide periods with no wind or rain, there is little or no movement of water in the marsh.

Transient conditions in the marsh are evidenced from the discharges measured October 25, 1983. More water leaves the marsh at both ends of Salt Bayou than enters the marsh at canal W-14. This is due to tidal ponding, which is the build-up of water in an area such as the marsh during high tide. Steady-state conditions were approached on August 26, 1983. A small discharge of 3.8 ft^3/s entered the marsh at the east end of Salt Bayou (table 1). Discharges at canal W-14 and the west end of Salt Bayou were not measured on this date due to the very slow velocities at these locations.

Table 2.--Wind data for the New Orleans International Airport, December 13-20, 1983

[Wind direction: Directions are those from which the wind is blowing, indicated in tens of degrees from true north: For example, 09 for east; 18 for south; 27 for west; 36 for north; and 00 indicates calm.
Wind Speed (mi/h): The observed average 1-minute value expressed in miles per hour]

December 13			December 14			December 15			December 16			December 17			December 18			December 19			December 20		
Time	Wind direction	Wind speed (mi/h)	Time	Wind direction	Wind speed (mi/h)	Time	Wind direction	Wind speed (mi/h)	Time	Wind direction	Wind speed (mi/h)	Time	Wind direction	Wind speed (mi/h)	Time	Wind direction	Wind speed (mi/h)	Time	Wind direction	Wind speed (mi/h)	Time	Wind direction	Wind speed (mi/h)
0052	00	0.0	0052	25	13.8	0055	21	4.6	0052	06	3.5	0052	05	11.5	0052	05	10.4	0055	04	11.5	0054	03	9.2
0153	07	5.8	0152	25	13.8	0153	23	3.5	0155	07	4.6	0152	05	13.8	0152	05	10.4	0152	02	8.1	0155	03	8.1
0255	04	3.5	0252	26	12.7	0252	21	5.8	0252	06	4.6	0252	04	10.4	0252	05	9.2	0255	01	10.4	0255	36	9.2
0354	04	3.5	0352	26	11.5	0352	21	5.8	0352	07	3.5	0352	04	12.7	0353	05	10.4	0355	03	8.1	0355	03	9.2
0452	09	4.6	0452	27	11.5	0452	22	5.8	0452	00	.0	0452	04	12.7	0452	04	8.1	0454	03	8.1	0455	36	9.2
0553	00	.0	0552	31	11.5	0552	22	6.9	0552	00	.0	0552	04	13.8	0552	05	9.2	0555	04	9.2	0555	03	9.2
0652	05	4.6	0652	27	9.2	0652	21	6.9	0652	06	3.5	0652	05	12.7	0653	03	9.2	0652	06	10.4	0654	03	8.1
0753	07	5.8	0752	26	8.1	0752	22	8.1	0752	05	8.1	0755	05	15.0	0752	04	10.4	0755	03	10.4	0755	03	10.4
0855	12	10.4	0855	26	11.5	0855	22	10.4	0855	06	11.5	0855	06	16.1	0855	04	10.4	0855	36	10.4	0855	03	9.2
0955	13	9.2	0955	26	12.7	0955	25	10.4	0955	07	16.1	0955	05	11.5	0955	05	8.1	0955	03	12.7	0955	03	12.7
1055	13	9.2	1055	29	13.8	1055	27	12.7	1055	08	18.4	1055	06	12.7	1055	05	8.1	1055	03	10.4	1055	03	10.4
1155	14	12.7	1155	30	10.4	1155	26	15.0	1155	07	12.7	1155	06	10.4	1155	05	8.1	1155	03	10.4	1155	05	10.4
1255	14	11.5	1255	30	6.9	1255	27	15.0	1253	06	9.2	1255	06	12.7	1255	05	10.4	1255	03	10.4	1255	36	8.1
1355	14	15.0	1355	25	4.6	1355	27	10.4	1355	07	12.7	1355	04	8.1	1355	05	8.1	1355	34	8.1	1355	04	9.2
1455	14	10.4	1455	26	6.9	1455	28	10.4	1455	07	11.5	1455	05	9.2	1455	05	6.9	1455	33	9.2	1455	04	10.4
1555	10	9.2	1555	26	6.9	1555	36	5.8	1555	06	11.5	1555	04	5.8	1555	03	6.9	1555	36	9.2	1555	05	9.2
1655	09	9.2	1655	29	4.6	1655	02	3.5	1653	06	16.1	1655	04	6.9	1654	04	8.1	1654	01	12.7	1652	04	8.1
1755	10	13.8	1755	30	6.9	1754	36	4.6	1752	06	15.0	1752	04	6.9	1753	04	12.7	1753	34	9.2	1752	05	8.1
1855	15	12.7	1854	29	8.1	1854	00	.0	1852	04	11.5	1851	04	8.1	1851	04	10.4	1854	36	9.2	1852	06	6.9
1955	23	13.8	1954	27	5.8	1954	02	3.5	1954	04	12.7	1951	04	8.1	1952	03	9.2	1953	36	9.2	1952	06	8.1
2055	23	13.8	2055	26	5.8	2055	10	3.5	2051	04	12.7	2052	04	9.2	2053	04	9.2	2053	03	9.2	2052	07	5.8
2155	24	12.7	2155	26	5.8	2154	00	.0	2152	04	9.2	2153	04	9.2	2152	04	13.8	2153	03	8.1	2152	05	5.8
2254	25	12.7	2254	26	4.6	2255	00	.0	2255	04	10.4	2253	05	8.1	2251	04	11.5	2253	04	10.4	2255	06	8.1
2317	25	12.7	2355	0	.0	2354	00	.0	2353	05	12.7	2353	06	8.1	2353	04	12.7	2353	04	10.4	2352	07	9.2

FRITCHIE MARSH MODEL DEVELOPMENT

The geometry and types of vegetation of Fritchie Marsh were determined by field measurements and aerial photographs. This information was incorporated into a network of triangular elements to develop a mathematical model of the marsh. A general description of the FESWMS program is included in the appendix. In this section of the report, the development of the finite-element network for Fritchie Marsh is discussed.

Network Design

The first task in applying the FESWMS program to a problem is to define the area to be modeled and develop a network of triangular elements over this area. For this study, the finite-element network was drawn on U.S. Geological Survey topographic maps enlarged to a scale of 1:2,400.

The network shown on plate 1 was designed to follow the irregular boundary of the marsh. The northwestern boundary starts south of Doubloon Branch and perpendicular to canal W-14 in a fully wetted part of the marsh. The remainder of the northern, eastern, and western boundaries of the modeled area are at the marsh perimeter where the land surface is above the water surface much of the time as determined from aerial photographs and topographic maps. The southwestern boundary follows the north side of the unnamed island mentioned earlier, the berm, a small private road to Prevost Island, and the north side of Prevost Island (fig. 2).

Once the boundary was defined, the model area was subdivided into triangular elements (pl. 1). Smaller elements were placed within channels; the channels modeled were canal W-14 and Salt Bayou. The Salt Bayou channel was represented as a straight channel to reduce the total number of elements used in the model. Once the channels were defined in the network, other areas were delineated by subdividing the marsh areas into places of similar vegetation and geometry. Details of the many small channels in the marsh were not included in the network. This network keeps the modeling effort within the scope of the project resources and provides sufficient detail of the marsh.

Sharp gradients in either velocity, depth, or water surface over a single triangular element may cause local inconsistencies in the numerical solution of the flow equations. For this reason, greater network detail was required where sharp changes in velocity, depth, or water surface were expected (along the channels and near the bridge opening at Louisiana Highway 433 and Salt Bayou).

The shape of the triangles may also affect solution of the equations. The element aspect ratio is defined as the ratio of the largest element dimension to the smallest. Optimum aspect ratios for a given element depend on the gradients of velocity, depth, and water surface over the element. Generally, the smallest element dimension should be aligned with the largest variable change and the largest element dimension with the smallest variable change (Lee and others, 1983). Elements with large aspect ratios were used in defining the channels. Elements were aligned with the largest dimension parallel to the flow path in the channel.

Each element contains six nodes (corresponding to the three vertices and the mid-points of the three sides). The number of nodes and elements in a model network determines the detail to which the model can simulate the system and also is related to the effort required for its development. The finite-element network, shown on plate 1, has 1,335 elements and 2,770 nodes.

Channel Geometry

During field investigation, channel cross sections were measured along canal W-14 and Salt Bayou. Triangular-channel cross sections are used in the model. The areas of the field cross sections determined the bottom elevation of the triangular channels used in the model, such that both areas were equivalent. In figure 5, the solid line shows a natural cross section of Salt Bayou, and the dashed line its equivalent model cross section. Linear interpolation was used between field cross sections for the model channel.

The length of canal W-14 was the same for the natural channel and the modeled channel, but Salt Bayou was shortened considerably in the model. This shortening of Salt Bayou was accounted for by adjusting the Chézy coefficient for the shortened channel using the following relationship:

$$C_s = (L_s/L_n)^{0.5} \qquad (1)$$

where C refers to the Chézy coefficient, L the length, and the subscripts s and n refer to shortened and natural channels, respectively (Lee and others, 1983).

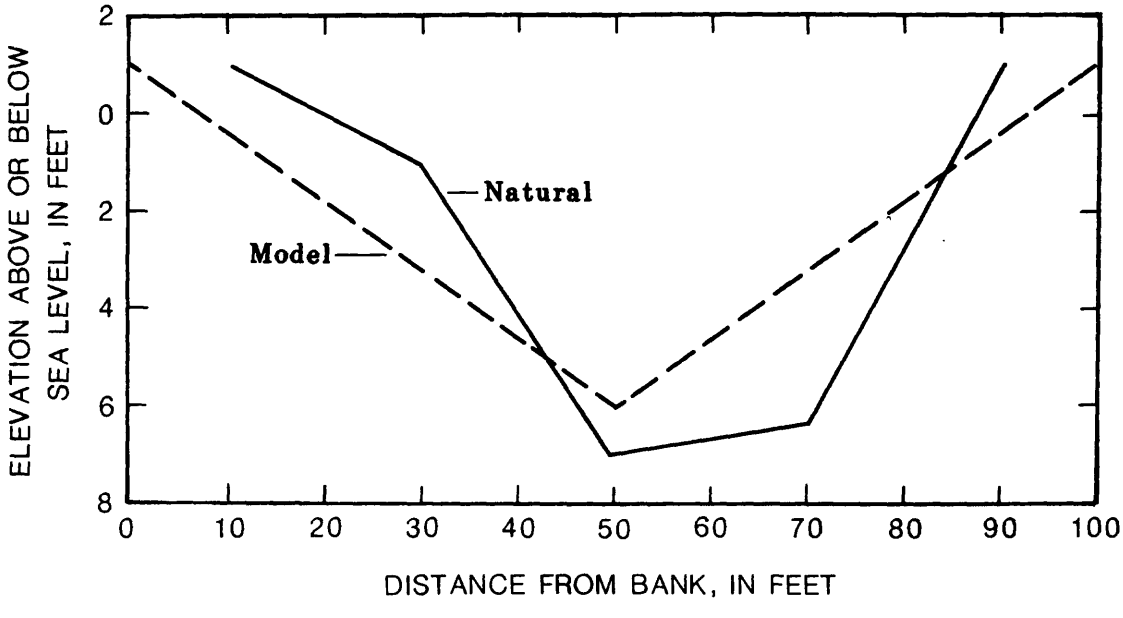

Figure 5.--Natural and equivalent model cross sections.

Element Property Types

Seven different element property types were designated in modeling Fritchie Marsh. They indicate different vegetation and roughness properties that are related to the Chézy discharge coefficients used for the model elements. These element types were also used to adjust roughness values in part of the marsh where small channels were not modeled. Plate 1 includes a table showing the seven different Chézy coefficients specified for each element property type.

Type 1 designates canal W-14 and parts of the marsh that are open water. Type 2 designates areas of the marsh that have some vegetation, such as lily pads. Type 3 designates areas having some marsh grass. Type 4 designates areas where the marsh grass is fairly thick. Type 5 designates elements that were placed at small islands in the marsh. The Chézy coefficient was set low to restrict flow over those elements. Types 6 and 7 designate the straightened parts of Salt Bayou and correspond to types 1 and 2, respectively, with Chézy coefficients reduced by a factor of 0.8885. This factor was obtained by using equation 1.

In the actual marsh, many small channels connect the large pond-like region to both canal W-14 and Salt Bayou. To allow for flow from the pond-like area to the modeled channels, increased discharge coefficients were used. On plate 1, the element property types are identified by patterns and numbers. In some places, element types 1 and 2 were used between the pond-like region and the channels.

No attempts to measure or verify the values of the Chézy coefficients were made. The values used in this model were adapted from the values for these coefficients used in modeling the lower Pearl River (Lee and others, 1983).

FRITCHIE MARSH SIMULATIONS

For this preliminary study of Fritchie Marsh, four steady-state simulations were run on the Louisiana District's PRIME minicomputer[2] using the FESWMS package. While steady-state simulations could not provide information on detention time or changes in storage of water in the marsh over a tidal cycle, the simulations did give insight into magnitudes of velocities in the marsh and flow patterns for selected hydrologic events. Two hydrologic conditions were simulated and were selected as events that were possible and that approach steady-state for a period of time in the marsh. Two inflow rates at canal W-14, representing present and future sewage effluent from Slidell, were superimposed on the two hydrologic events.

---

[2] Use of trade names in this report is for identification purposes only and does not constitute endorsement by the U.S. Geological Survey or the Louisiana Department of Environmental Quality.

Simulated Hydrologic Events and Boundary Conditions

The first hydrologic event simulated was a neap tide with no prevailing winds over the Gulf Coast region and no significant rainfall over the lower Pearl River basin. This event is possible at Fritchie Marsh and would be a worst-case hydrologic condition for mixing in the marsh. For the simulations of this event the water-surface elevation was set at 1.0 ft above sea level over the whole marsh. This was the observed water-surface elevation (1.0 $\pm$ 0.3 ft) at the marsh during the week of August 22-26, 1983.

The second event simulated was a higher tide with a difference in water-surface elevation of 0.5 ft from east to west on Salt Bayou and no significant rainfall over the lower Pearl River basin. The water-surface elevations were set at 1.8 and 2.3 ft above sea level at the east and west ends of Salt Bayou, respectively. The cause of such an event could be low stage on the West Pearl River and a strong prevailing wind from the southeast creating a higher water elevation in Lake Pontchartrain than at the West Pearl River. In figures 3b and 3c it can be seen that the water-surface elevations at the east and west sides of the marsh were not the same at all times. There currently is no record of a prolonged period during which the difference in water level at both sides of the marsh were the same; therefore, the steady-state assumption may not be as valid for this event as for the neap tide with no wind event.

For both hydrologic events, stage was specified at each end of Salt Bayou and discharge into the marsh was specified at canal W-14. All other boundaries were treated as slip boundaries which allow tangential flow along the edges of the marsh.

Inflows at Canal W-14

Canal W-14 drains a small area and flow in the canal is due to storm runoff, base flow, and sewage effluent. For the simulations in this study, the minimum and maximum inflows were base flow with existing sewage-effluent flow, and base flow with projected sewage-effluent flow, respectively. The existing sewage-effluent flow in canal W-14 is 5.7 Mgal/d (8.8 ft^3/s). Future development plans by the city of Slidell show a maximum average rate of 11.8 Mgal/d (18.3 ft^3/s) of sewage effluent discharged to canal W-14.

Base flow was estimated by subtracting the existing sewage-effluent flow of 8.8 ft^3/s from the 23 ft^3/s discharge measurement made on October 25, 1983, yielding about 14 ft^3/s of base flow. The minimum inflow input at the north end of canal W-14 was 23 ft^3/s (base flow plus 8.8 ft^3/s sewage effluent) and the maximum was about 32 ft^3/s (base flow plus 18.3 ft^3/s sewage effluent). These were input as unit discharges across the width of the boundary of canal W-14.

Simulation Results

Plates 2 and 3 show the flow directions from the model simulations of neap tide with no significant rainfall over the lower Pearl River basin and no prevailing winds in the Gulf Coast region. Plate 2 shows the results for minimum sewage effluent and plate 3 for maximum sewage effluent entering the marsh at canal W-14. Arrows represent the velocity vectors at each node greater than or equal to 0.001 ft/s. (Velocities less than 0.001 ft/s cannot be measured with velocity meters and, thus, are considered to be zero.) The density of the arrows on these plates in no way corresponds to flow rates. A higher density of arrows indicates a finer finite-element network, such as along channels and at the bridge opening in Louisiana Highway 433. The general flow directions for both simulations were very similar, but the distribution of the three ranges of velocities shown varied. With minimum inflow at canal W-14, velocities over the entire marsh were lower in magnitude than for the maximum inflow simulation. The only place where velocities were greater than 0.01 ft/s in either simulation was where inflow from canal W-14 entered the marsh and near the boundary cross section at the end of canal W-14. This flow left canal W-14 through the smaller channels, simulated by raising the Chézy coefficients of elements at the channel boundary, and went into the marsh and southward to Little Lagoon, exiting through the bridge opening at Louisiana Highway 433.

For the simulation of neap tide, most of the water entering the marsh leaves through the bridge opening on Louisiana Highway 433. As shown on plates 2 and 3, the marsh has predominantly stagnant water on its east side. Flow directions along Salt Bayou were westward towards the bridge opening except at maximum inflow adjacent to the culvert opening at U.S. Highway 90 and Salt Bayou.

The second hydrologic event simulated had a higher tide with a higher water-surface elevation in Lake Pontchartrain than the West Pearl River and no significant rainfall over the lower Pearl River basin. The results of the simulations of minimum sewage effluent for this event are shown on plate 4 and figure 6. Plate 4 shows the flow pattern and figure 6 shows water-stage contours for the simulation with minimum inflow at canal W-14. The maximum inflow simulation is not shown because flow patterns and water stage are similar to the minimum inflow simulation.

Because of the higher water-surface elevation imposed at Salt Bayou at Louisiana Highway 433, water entered the marsh at the bridge opening on Louisiana Highway 433 and left the marsh through the culvert opening in U.S. Highway 90 at Salt Bayou. The 0.5-foot drop in water-surface elevation, from the bridge opening in Louisiana Highway 433 to the culvert opening in U.S. Highway 90, created different circulation patterns in the marsh (pl. 4); but velocities were still very slow for these two simulations. For this second hydrologic event, velocities greater than 0.01 ft/s occur at the inflow point on canal W-14 and at the outflow point where flow leaves the marsh at the culvert opening on U.S. Highway 90 at Salt Bayou. There is less stagnant water on the east side of the marsh,

but slower velocities at the west side of the marsh near Louisiana Highway 433. The flow restriction at the north end of canal W-14 still affects the flow direction; water entering the marsh at canal W-14 moves eastward through the marsh.

Over most of the marsh, the stage is 2.3 ft above sea level except near the culvert at Salt Bayou at U.S. Highway 90 where the stage drops to 1.8 ft. (See fig. 6.) The stage contours for both simulations of the hydrologic event are identical. All of the flow passes out of the marsh through the node used to simulate the culvert resulting in the drop in water surface around the culvert.

Discussion of the Simulations

The first hydrologic event simulated was the neap-tide period with no prevailing winds or rain in the area as observed on August 26, 1983. A steady-state assumption for this event was appropriate. The second event, with the tide differential of 0.5 ft, was not observed at the marsh but was considered possible. A steady-state assumption for this event was not as accurate because the higher tide, with wind causing a 0.5-foot difference in water-surface elevation on each side of the marsh, may not occur for a long enough period of time for steady-state conditions to be established in the marsh.

The two hydrologic events simulated are not the only possible conditions at Fritchie Marsh, but were believed to be two of the worst possible conditions affecting mixing in the marsh. Neap tides occur every 14 days, but no analysis of wind or precipitation data was done to determine the probability of the occurrence of the hydrologic conditions simulated for this preliminary study.

The model developed for Fritchie Marsh has not been calibrated and the results cannot be verified with existing stage and discharge data. Fairly good data were obtained to establish the geometry of the marsh and aerial photographs were very useful for establishing the location of different vegetation types in the marsh. The values of the Chézy coefficients used in the model for different vegetation areas were taken from the calibrated model of the lower Pearl River (Lee and others, 1983). Therefore, there is confidence that the model simulations presented in this report give a general concept of the flow patterns in the marsh for these worst-case hydrologic events.

DATA COLLECTION PROCEDURES FOR FUTURE INVESTIGATION

Calibrated hydrodynamic simulations of the marsh using the model developed for this study would require the gathering of stage and discharge data at the marsh. Continuous recording gages at four locations: (1) canal W-14 at Voters Road, (2) Salt Bayou at Louisiana Highway 433, (3) Salt Bayou at U.S. Highway 90, and (4) somewhere in the middle of the marsh would be necessary for determining stage fluctuations at the inflow-outflow boundaries and inside the marsh. Discharge data collected with a directional-velocity meter at the first three recording-gage

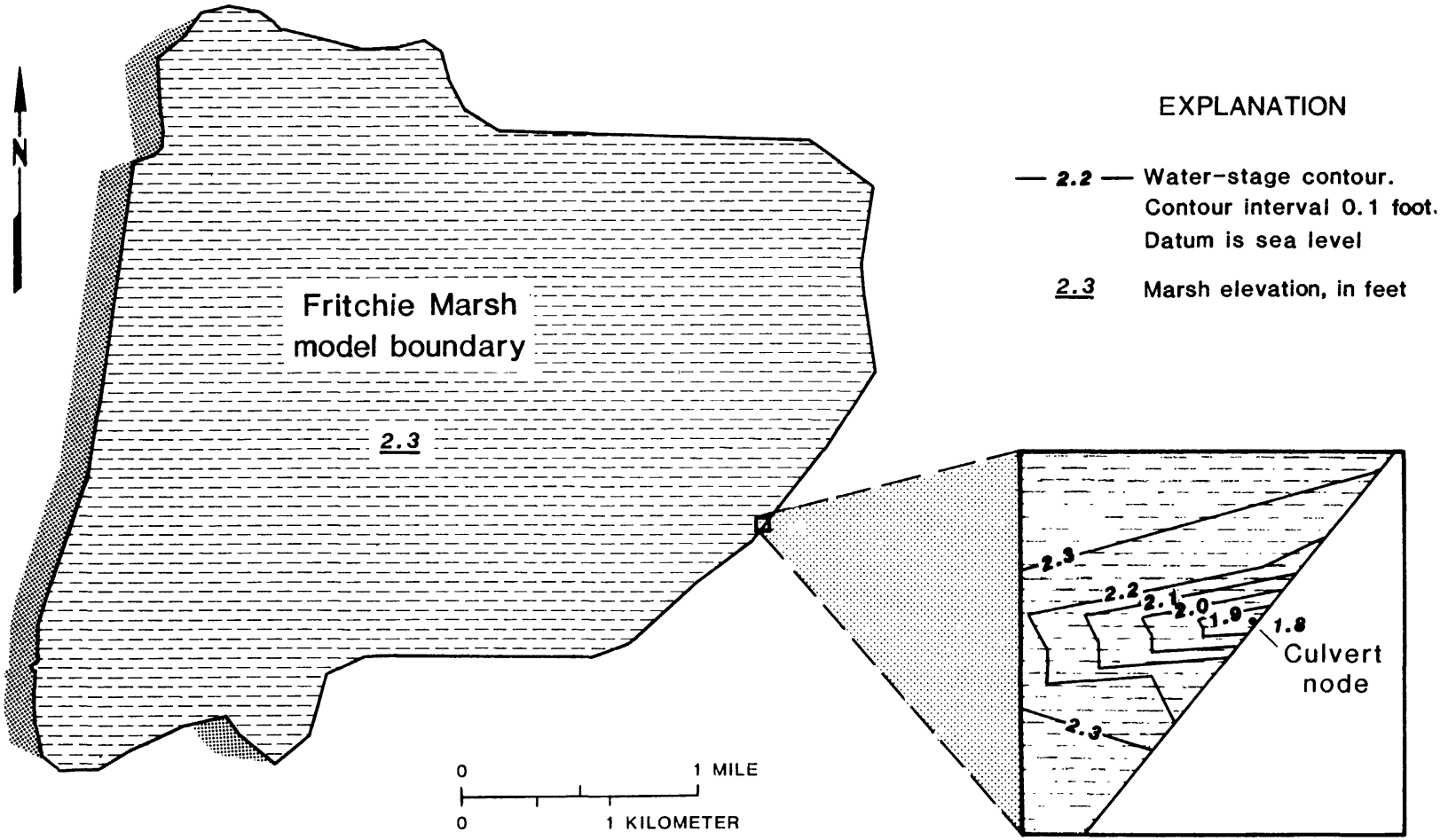

Figure 6.--Water-stage contours for simulation of high tide with tide differential.

locations would be useful for defining the discharges at these boundaries. Wind data collected near the marsh would be used for comparisons with wind data from the New Orleans International Airport and in determining the correlation of wind stress with stage variation.

All the the data collected simultaneously could be used for both the model calibration and hydrodynamic simulation. This field-intensive effort could be made during a period of little or no precipitation and also during a rainy period in order to define the hydraulics of the marsh during different meteorological conditions, but avoiding extreme conditions such as hurricanes and floods.

CONCLUSIONS

The factors affecting flow patterns in Fritchie Marsh are the stage of the West Pearl River, gravity tides along the Mississippi and Louisiana coast, strong prevailing winds in the Gulf Coast region, precipitation over the lower Pearl River basin, and sewage effluent in canal W-14. For this study a two-dimensional mathematical model of Fritchie Marsh was developed to approximate flow patterns within the marsh for specific hydrologic events. Because of the interest in the sewage-assimilation capability of the marsh, the two events simulated by the model were selected as events that were possible and that would create some of the worst conditions in the marsh for assimilation of treated domestic sewage.

The simulations showed that, during periods of little or no rainfall, velocities in the marsh may be very low. Also, during a neap-tide period with no wind-induced flow at the marsh, a large part of the marsh was virtually stagnant, especially the eastern side of the marsh away from canal W-14. If the water surface in Lake Pontchartrain were higher than in the West Pearl River, velocities in the marsh would be larger; but without significant rainfall, the velocities would still be small. There was very little difference in flow patterns in the marsh between minimum and maximum sewage effluent in canal W-14 for either of the two hydrologic conditions.

With more data, the model of Fritchie Marsh could be calibrated, and other weather-related situations could be simulated. The utility of this model in defining the factors affecting water movement in the marsh has been demonstrated by this preliminary study and specific needs for collecting data for future investigations were determined.

REFERENCES CITED

Cardwell, G. T., Forbes, M. J., Jr., and Gaydos, M. W., 1967, Water resources of the Lake Pontchartrain area, Louisiana: Louisiana Department of Conservation and Louisiana Department of Public Works Water Resources Bulletin 12, 105 p.

Chow, V. T., 1959, Open-channel hydraulics: New York, McGraw-Hill, 680 p.

Gee, D. M., and MacArthur, R. C., 1978, Development of generalized free surface flow models using finite element techniques, in Brebbia, C. A., and others, eds., Finite elements in water resources: Second International Conference on Finite Elements in Water Resources, London, 1978, Proceedings: London, Pentech Press, p. 2.61-2.79.

Hood, P., 1976, Frontal solution program for unsymmetric matrices: International Journal for Numerical Methods in Engineering, v. 10, no. 2, p. 279-399.

King, I. P., and Norton, W. R., 1978, Recent applications of RMA's finite element models for two-dimensional hydrodynamics and water quality, in Brebbia, C. A., and others, eds., Finite elements in water resources: Second International Conference on Finite Elements in Water Resources, London, 1978, Proceedings: London, Pentech Press, p. 2.81-2.99.

Lee, J. K., Froehlich, D. C., Gilbert, J. J., and Wiche, G. J., 1983, A two-dimensional finite-element model study of backwater and flow distribution at the I-10 crossing of the Pearl River near Slidell, Louisiana: U. S. Geological Survey Water-Resources Investigations Report 82-4119, NSTL Station, Miss., 60 p.

Norton, W. R., and King, I. P., 1973, A finite element model for Lower Granite Reservoir, computer application supplement and user's guide: Walnut Creek, Calif., Water Resources Engineers, Inc., 90 p.

Norton, W. R., King, I. P., and Orlob, G. T., 1973, A finite element model for Lower Granite Reservoir: Walnut Creek, Calif., Water Resources Engineers, Inc., 138 p.

Pritchard, D. W., 1971, Two-dimensional models, in Ward, G. H., Jr., and Espey, W. H., Jr., eds., Estuarine modeling: An assessment: Environmental Protection Agency, Water Quality Office, Water Pollution Control Research Ser. 16070DZV, p. 22-33.

Tseng, M. T., 1975, Evaluation of flood risk factors in the design of highway stream crossings. v. III. Finite element model for bridge backwater computation: Federal Highway Administration Report No. FHWD-RD-75-53, 176 p.

Walters, R. A., and Cheng, R. T., 1978, A two-dimensional hydrodynamic model of a tidal estuary, in Brebbia, C. A., and others, eds., Finite elements in water resources: Second International Conference on Finite Elements in Water Resources, London, 1978, Proceedings: London, Pentech Press, p. 2.3-2.21.

----- 1980, Accuracy of an estuarine hydrodynamic model using smooth elements: Water Resources Research, v. 16, no. 1, p. 187-195.

Zienkiewicz, O. C., 1977, The finite element method (3d ed.): London, McGraw-Hill, p. 200-201.

APPENDIX

The Finite-Element Surface-Water Modeling System Program

(This section is modified from Lee and others, 1983)

The core of the two-dimensional FESWMS program is based on the works of Norton and King (1973); Norton, King and Orlob (1973); Tseng (1975); and King and Norton (1978). Around this core, the Geological Survey has developed preprocessing and postprocessing programs which make the flow model more usable. Preprocessing programs place input data in an appropriate form for the flow model and plot maps of finite-element networks and associated data. Postprocessing programs plot maps of velocity vectors, water-surface contour lines, backwater contour lines, discharge at specified cross sections, and established water stage.

The formulation and development of the flow model have been described elsewhere; therefore, only the equations solved and a brief outline of the technique used to solve them are presented here.

Flow Equations

Under the usual assumptions (for example, hydrostatic pressure and equating to one the momentum correction factors), two-dimensional surface-water flow in the horizontal plane is described by three nonlinear partial-differential equations, two for conservation of momentum and one for conservation of mass (Pritchard, 1971):

$$\frac{\partial u}{\partial t} + u\frac{\partial u}{\partial x} + v\frac{\partial u}{\partial y} + g\frac{\partial h}{\partial x} + g\frac{\partial z_o}{\partial x} - \frac{1}{\rho h}\left[\frac{\partial}{\partial x}\left(\epsilon_{xx} h \frac{\partial u}{\partial x}\right) + \frac{\partial}{\partial y}\left(\epsilon_{xy} h \frac{\partial u}{\partial y}\right)\right]$$

$$- 2\omega v \sin\phi + \frac{gu}{C^2 h}(u^2 + v^2)^{1/2} - \frac{V_a^2}{h}\cos\quad = 0, \qquad (1)$$

$$\frac{\partial v}{\partial t} + u\frac{\partial v}{\partial x} + v\frac{\partial v}{\partial y} + g\frac{\partial h}{\partial y} + g\frac{\partial z_o}{\partial y} - \frac{1}{\rho h}\left[\frac{\partial}{\partial x}\left(\epsilon_{yx} h \frac{\partial v}{\partial x}\right) + \frac{\partial}{\partial y}\left(\epsilon_{yy} h \frac{\partial v}{\partial y}\right)\right]$$

$$+ 2\omega u \sin\phi + \frac{gv}{C^2 h}(u^2 + v^2)^{1/2} - \frac{V_a^2}{h}\sin\quad = 0, \qquad (2)$$

and

$$\frac{\partial h}{\partial t} + \frac{\partial}{\partial x}(uh) + \frac{\partial}{\partial y}(vh) = 0, \qquad (3)$$

where

C = Chézy coefficient (feet to the one-half power per second),
g = gravitational acceleration (feet per second squared),
h = depth (feet),
t = time (seconds),
u, v = depth-averaged velocity components in the x- and y-directions, respectively (feet per second),
x, y = Cartesian coordinates in the positive east and north directions, respectively (feet),
V_a = local wind velocity (feet per second),
z_o = bed elevation (feet),
$\varepsilon_{xx}, \varepsilon_{xy}, \varepsilon_{yx}, \varepsilon_{yy}$ = eddy viscosities (pound second per square foot),
ζ = water-surface resistance coefficient (nondimensional),
ρ = density of water (assumed constant) (slugs per cubic foot),
ϕ = latitude (degrees),
ψ = angle between the wind direction and the x-axis (degrees), and
ω = rate of the Earth's angular rotation (per second).

The two-dimensional surface-water flow equations account for energy losses through two mechanisms: bottom friction and turbulent stresses. The Chézy equation for bottom friction in open-channel flow is extended to two dimensions for use in equations 1 and 2. Equations 1 and 2 also use Boussinesq's eddy-viscosity concept, which assumes the turbulent stresses to be proportional to the mean-velocity gradients.

Boundary conditions consist of the specification of flow components or water-surface elevations at open boundaries and zero flow components or zero normal flow (tangential flow) at all other boundaries, called lateral boundaries. For a time-dependent problem, initial conditions must also be specified. Equations 1 through 3, together with properly specified boundary and initial conditions, make up a well-posed initial-boundary-value problem.

Numerical Solution of the Flow Equations

Quadratic basis functions are used to interpolate velocity components, and linear basis functions are used to interpolate depth on triangular, six-node, isoparametric elements (mixed interpolation). Model topography is defined by assigning a ground-surface elevation to each element vertex and requiring the ground surface to vary linearly within an element.

The finite-element model requires the specification of a constant Chézy coefficient, C, and a constant symmetric turbulent-exchange, or eddy-viscosity, tensor, ε, over each element. Nonisotropic turbulent stresses can be simulated by assigning different values to the components of the eddy-viscosity tensor. The eddy-viscosity terms in the momentum equations suppress nonlinear instabilities generated by the convective terms, and nonzero eddy-viscosity values are necessary for convergence of

the numerical method to a solution. The eddy-viscosity values can influence the results of a simulation; however, optimum values are difficult to determine. In general, increased values serve to increase water-surface slopes. It is also known that eddy-viscosity values should increase with element size.

Flow components are specified at inflow boundary nodes, and water-surface elevations are specified at outflow boundary nodes. In this study, zero normal flow was specified at all lateral boundaries. Isoparametric elements permit the use of smooth, curved lateral boundaries. The improvement in accuracy obtained by using such boundaries, together with the specification of zero normal flow (tangential flow) there, has been documented by Gee and MacArthur (1978), King and Norton (1978), and Walters and Cheng (1978, 1980) for the mixed-interpolation formulation of the surface-water flow equations.

Galerkin's method of weighted residuals, a Newton-Raphson iteration scheme, numerical integration using seven-point Gaussian quadrature (Zienkiewicz, 1977, p. 200-201), and a frontal solution algorithm using out-of-core storage (Hood, 1976) are used to solve for the nodal values of the velocity components and depth. The time derivatives are handled by an implicit finite-difference scheme; in the application reported here, however, only the steady-state forms of the equations were solved.

If a finite-element network is not well designed, errors in conservation of mass can be significant, because there are only approximately half as many equations for conservation of mass as there are for conservation of momentum in either the x- or y-direction. For a well-designed network, however, errors in mass conservation are small. The model has the capability of integrating the discharge across a line (called continuity checks) following element sides and beginning and ending at element vertices. Thus, conservation of mass can be checked (King and Norton, 1978).

Gee and MacArthur (1978) completed a cursory study of continuity check errors with a two-dimensional finite-element model similar to the one used in this study. They concluded that a steady-state solution is acceptable if the discharge at all continuity checklines does not deviate from the input discharge by more than ± 5 percent.